# Filament spinning of unbleached birch kraft pulps: Effect of pulping intensity on the processability and the fiber properties

Yibo Ma[a], Jonas Stubb[a], Inkeri Kontro[b], Kaarlo Nieminen[a], Michael Hummel[a], Herbert Sixta[a].

[a]     Y. Ma, Dr. M. Hummel, Prof. H. Sixta

        Department of Forest Products Technology

        School of Chemical Technology

        Aalto University

        P.O. Box 16300, 00076 Aalto (Finland)

        E-mail: herbert.sixta@aalto.fi

[b]     I. Kontro.

        Division of Material physics, Department of Physics

        Helsinki University

        P.O. Box 64, FI-00014, (Finland)

Highlights

- Man-made fibres were spun from low refined kraft pulps.
- E-beam as dry, non-chemical treatment was used for DP adjustment of lignocellulose.
- The effect of the chemical compositions on the spinnability is only minor.
- The spinnability is mainly dependent on the molecular integrity of lignocellulose matrix.

**ABSTRACT** Man-made lignocellulosic fibres were successfully prepared from unbleached birch kraft pulps by using the IONCELL-F technology. Pulps with different lignin content were produced by tailored kraft pulping with varying intensity. The degree of polymerization of the pulps was adjusted by acid-catalyzed hydrolysis and electron beam treatment. All substrates were completely soluble in 1,5-diazabicyclo[4.3.0]non-5-enium acetate ([DBNH]OAc) and the respective solutions were spinnable to yield fibres with good to excellent mechanical properties despite the use of only mildly refined wood pulp. The tensile properties decreased gradually as the lignin concentration in the fibres increased. Changes in the chemical composition also affected the structure and morphology of the fibres. Both the molecular orientation and the crystallinity decreased while the presence of lignin enhanced the water accessibility. The effects of the crystallite size and lignin content on monolayer water adsorption are discussed.

*Keywords*: *Lignocellulose, fibres, refining, spinning, ionic liquid.*

## 1. INTRODUCTION

The global demand of textile fibres is gradually increasing in response to the global megatrends such as population and prosperity growth in combination with sustainability thinking and the limited increase in the production capacities of cotton. Thus, more man-made cellulosic fibres (MMCFs) are potentially needed to fill the 'fibre demand gap' in the future (Hämmerle, 2011). Currently, the major markets of MMCFs are dominated by viscose and Lyocell fibres. However, the viscose fibre process is connected to environmental and safety concerns due to the utilization of $CS_2$ for the intermediate derivatization of cellulose into cellulose xanthate (Hermanutz, Meister, & Uerdingen, 2006). In addition to the mentioned drawbacks of this process, this technology demands dissolving pulp as feedstock. In the viscose process, the presence of lignin and hemicellulose will deteriorate the xanthation of the pulp and process filterability drastically. This results in poor spinnability, if processable at all (Hans Peter Fink et al., 2004; Gübitz, Stebbing, Johansson, & Saddler, 1998). The Lyocell process is an environmentally friendly process in which both the cellulose solvent and spent water are fully recovered and circulated. This process allows for the direct dissolution of cellulose to yield a spin dope that is processed through dry-jet wet spinning. The spun fibres are clearly stronger than regular viscose fibres. Despite the advantages of the Lyocell process, the process operates at a relatively high temperature and requires the addition of stabilizers to prevent dangerous runaway reactions during the dope preparation and spinning (H P Fink, Weigel, Purz, & Ganster, 2001). From the feedstock point of view, the NMMO-based Lyocell process can already utilize dissolving pulp, paper grade pulp (with high hemicellulose content) and even unbleached chemical pulp for fibre production (Rosenau, Potthast, Sixta, & Kosma, 2001). However, NMMO, as an oxidant, might react with the lignin present in the raw material to unexpected degradation reaction, especially at high temperatures between 110 and 130 ºC as typically used in the NMMO process. Furthermore, the dissolution of

60 the raw material in NMMO could be more difficult, thus affecting the quality of the dope which

61 may lead to spinnability problems (Hans Peter Fink et al., 2004).

62 The IONCELL-F process is a recently developed process in which the ionic liquid 1,5-

63 diazabicyclo [4.3.0]non-5-enium acetate ([DBNH][OAc]) is utilized as a solvent for cellulosic

64 material and the resulting dope is processed in a dry jet-wet spinning process to form filaments

65 with high mechanical properties (Hummel et al., 2015; A Michud et al., 2014; Parviainen et al.,

66 2013; Sixta et al., 2015). The IONCELL-F process, a Lyocell-type fibre process, is considered to

67 be a green fibre spinning technology. It has been shown that it is largely insensitive to the

68 composition of lignocellulosic material and tolerates varying amounts of non-cellulosic

69 components such as lignin and hemicelluloses (Y Ma et al., 2016; Yibo Ma et al., 2015a). Thus, it

70 is not necessary to source highly refined dissolving pulp for this spinning process.

71 In previous studies (Le, Ma, Borrega, & Sixta, 2016; Y Ma et al., 2016), we have demonstrated

72 the possibility to spin unbleached organosolv pulps, waste fine paper and pre-treated waste

73 cardboard in IL solution and the spun fibres showed good to excellent properties. However,

74 untreated waste cardboard (made from mainly low-refined semi-chemical pulp), which contains a

75 large lignin content, cannot be dissolved in the IL completely. The spinning dope resulting from

76 the untreated waste cardboard behaves likes a gel, which can only be spun with low draw ratio and

77 the fibre properties were unacceptably low for commercial and technical applications. Jiang et

78 al.(Jiang, Sun, Hao, & Chen, 2011) and Sun et al.(Sun et al., 2011) have also reported the

79 possibility of spinning fibres from lignocellulosics using IL as a solvent. However, due to the

80 presence of lignin and hemicellulose, the spun fibres showed rather low mechanical properties, not

81 suitable for commercial use. To confirm the negative effect of native lignin on the solubility and

82 spinnability, polymer blends of cellulose and lignin with different ratio were subjected to

83  dissolution and fibre spinning (Yibo Ma et al., 2015a). Different to the native lignocellulosic

84  material, the polymer blends with up to 50% lignin can be readily dissolved in IL and the fibres

85  produced from the IL – polymer dope show good mechanical properties. Presumably, lignin

86  molecules embedded in the cell wall architecture are associated with polysaccharides, mainly

87  hemicellulose, forming lignin-carbohydrate complexes (LCCs), which hamper the complete

88  dissolution of the native lignocellulosics in IL and leads to a gel-like solution, respectively (Hauru

89  et al., 2013; Sun et al., 2009).

90      The main objectives of the study at hand are to investigate the spinnability of unbleached,

91  hemicellulose-rich kraft pulps from birch wood. The primary goal is to identify the critical content

92  of native lignin at which the pulp cannot be dissolved efficiently in an IL solvent and thus, results

93  in poor spinnability. The findings from this research work provide valuable information on the

94  necessary minimum refining degree for the dry-jet wet spinning of lignocellulosic material.

95

## 2. Experimental Section

### 2.1 Kraft cooking

98  Birchwood (*Betula pendula*) chips were provided by Metla, Finland. The dissolving grade birch

99  prehydrolyzed kraft (PHK) pulp (Enocell Pulp) was kindly supplied by Stora Enso, Finland. The

100 birchwood chips were screened according to standard SCAN-N 2:88 prior to kraft cooking. The

101 cooking was executed in 2 L autoclaves attached in a rotary air bath digester. The cooking

102 conditions are list in Table S1. Pulp samples were taken at H-factor (Sixta, 2006) 25, 50, 200, 500,

103 800, 1000 and 1200. These samples will be referred to as H25, H50 etc. After kraft cooking, the

104 black liquor was removed and the pulps were washed. The kraft pulps H1200, H1000, H800 and

105 H500 were subjected to screening with a Mänttä flat screen using a screen plate with a slot width

106  of 0.35 mm. The screening rejects were collected from the screen plate and dried in an oven at 105

107  ℃ for the determination of the rejects content. Due to the low degree of refining, the pulps H200,

108  H50 and H25 could not be defibrillated manually. Thus, a disc refiner was utilized for pulp

109  defibration. These samples were not screened due to the large amount of oversize fibers.

110  **2.2 Degree of polymerization (DP) adjustments**

111  The DP of the refined material was adjusted using two methods: acid-catalyzed hydrolysis and

112  electron beam (E-beam) irradiation treatment. The acid-catalyzed hydrolysis was done in the same

113  autoclave as was used for the kraft cooking. 5 samples, derived from H1200, H1000, H800, H500

114  and H200, were selected for the acid-catalyzed hydrolysis. The hydrolysis was accomplished for

115  2 hours at 130 ℃ with an acid concentration of 6 g/l. The samples were then washed and air-dried

116  for further use.

117  Birch PHK, birch H50 and birch H25 pulps were irradiated at LEONI Studer AG, Switzerland,

118  with a 10 MeV Rhodotron TT300 accelerator built by IBA for DP adjustment. Prior to E-beam

119  treatment, pulp sheets (thickness is 0.15 mm for each sheet) were prepared using a laboratory sheet

120  former. For establishing a dosage-DP relationship, the E-beam dosages were varied from 5 to 30

121  kGy for the different pulps. The large batch treatment for H25 and H50 pulps was performed at an

122  E-beam dosage of 20 kGy.

123  **2.3 Pulp dissolution**

124  [DBNH][OAc] was first melted at 70 ℃, then blended with the air-dried pulp (ground with a

125  Willey mill with 1 mm mesh sieves), stirred for 1.5 h at 80 ℃ with 10 rpm at reduced pressure

126  (50–200 mbar) using a vertical kneader system. The polymer concentration of the dope was

127  adjusted to 13 or 15 wt% according to the intrinsic viscosity of the pulps. The solutions were

128  filtered through a hydraulic press filter device (metal filter mesh with 5 µm absolute fineness, Gebr.

129  Kufferath AG, Germany) at 2 MPa and 80 ºC to remove undissolved substrate, which would lead

130  to unstable spinning. The prepared dope was finally shaped into the dimensions of the spinning

131  cylinder and solidified upon cooling overnight to ensure filling without inclusion of air bubbles.

## 2.3 Spinning trials

133  Multi-filaments were spun with a customized laboratory piston spinning system (Fourné

134  Polymertechnik, Germany). The solidified spinning dope was heated to 70 ºC in the spinning

135  cylinder to form a highly viscous, air-bubble-free spinning dope. The molten solution was then

136  extruded through a 36-hole spinneret with a capillary diameter of 100 μm and a length to diameter

137  ratio (L/D) of 0.2. After the generated filaments had passed an air gap of 10 mm, they were

138  coagulated in a water bath (10 to 15 ºC) in which they were guided by Teflon rollers to the godet

139  couple. The extrusion velocity ($V_e$) was set to 1.6 ml/min (5.66 m/min), while the take-up velocity

140  ($V_t$) of the godet was varied from 5 to 85 m/min to reach the maximum draw ratio (DR= $V_t/V_e$) at

141  which stable spinning was ensured. The fibres were washed off-line in hot water (60 °C) and air-

142  dried. The analytical methods of the raw materials, spinning dopes and spun fires including  were

143  carried out according to Yibo Ma et al. (2015b) and were presented in ESI section 1.

# 3. Results and Discussion

## 3.1 Pulp properties

146    To obtain pulps with different lignin content, seven birch wood kraft pulps (from H-factor 1200

147  to 25) were produced by means of a conventional kraft cooking method. As expected (and shown

148  in Table S1), the pulp yield before screening decreases as the H-factor increases. Pulp screening

149  was not possible for low refined pulps H25, H50, H200 due to incomplete defibration. Therefore,

150  the yield after screening could not be determined. The intrinsic viscosity of the different pulp

151  samples was almost at the same level. A significant reduction in viscosity was observed for H25

152 and 50. This is likely an artifact resulting from the low refining which prevents the dissolution of

153 high molecular weight fractions of pulp in CED.

154     Birch wood kraft pulps from H200 to H1200 were subjected to acid catalyzed hydrolysis in order

155 to reduce the intrinsic viscosity (optimal range 420 to 450 ml/g), which has been identified earlier

156 as optimum viscosity level to yield spinnable solutions. Table 1 lists the intrinsic viscosity ($\eta_0$) of

157 the pulps before and after the hydrolysis. The viscosity of the pulps was efficiently reduced by

158 acid catalyzed hydrolysis, albeit to a slightly lower level than initially aimed at. Concomitantly,

159 low molecular weight hemicelluloses were also degraded to such an extent that they became

160 soluble in the reaction liquor (Mosier et al., 2005). These phenomena were reflected by the MMD

161 as shown in Figure S1. Untreated pulps revealed a bimodal MMD (representing low-molecular

162 weight hemicellulose and high-molecular weight cellulose). However, as expected, after acidic

163 hydrolysis and further conversion to regenerated fibers (through dissolution in IL and regeneration

164 during the spinning process) the low molar mass peaks almost disappeared, leaving a cellulose

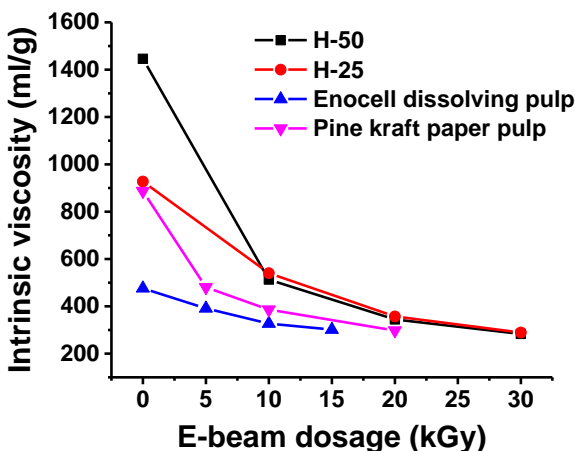165 peak with a subtle shoulder at relatively low molar mass.

166

167     **Table 1**. Intrinsic viscosity and chemical compositions of the original and DP adjusted kraft

168 pulps and their spun fibres.

| | Original kraft pulp | | | | DP adjusted pulps | | | | Fibres | | |
|---|---|---|---|---|---|---|---|---|---|---|---|
| Samples | Cellulose | Hemicellulose | Lignin | $\eta_0$ ml/g | Cellulose | Hemicellulose | Lignin | $\eta_0$ ml/g | Cellulose | Hemicellulose | Lignin |
| H25 | 53.7 | 22.4 | 23.9 | - | - | - | - | - | 55.8 | 20.2 | 24.0 |
| H50 | 56.4 | 21.8 | 21.8 | - | - | - | - | - | 57.9 | 21.7 | 20.4 |
| H200 | 63.6 | 21.9 | 14.5 | 1795 | 75.1 | 9.8 | 15.1 | 361 | 75.2 | 6.1 | 18.7 |
| H500 | 68.9 | 22.5 | 8.6 | 1591 | 83.6 | 7.9 | 8.5 | 390 | 85.9 | 5.2 | 8.9 |
| H800 | 71.2 | 23.0 | 5.8 | 1626 | 84.6 | 10.4 | 5.0 | 367 | 88.5 | 6.9 | 4.6 |
| H1000 | 72.0 | 22.6 | 5.4 | 1656 | 85.0 | 10.2 | 4.8 | 403 | 88.1 | 8.0 | 3.9 |
| H1200 | 72.7 | 22.2 | 5.1 | 1599 | 85.9 | 9.8 | 4.3 | 351 | 87.8 | 7.2 | 5.0 |

169

170     The chemical composition of the initial kraft pulps, the DP adjusted pulps, and the spun fibres

171     are summarized in Table 1. The hemicellulose content of acid hydrolyzed pulps is notably lower

172     than in the kraft pulps. Furthermore, there is a slight decrease in the lignin content. The reduction

173     in the hemicellulose and lignin contents result in a rise in the relative cellulose concentration of

174     the pulp, which facilitates the subsequent fiber spinning.

175     Birchwood kraft pulps H25, H50 were subjected to electron beam irradiation treatment. Electron

176     beam irradiation is an environmental friendly pre-treatment technology for lignocellulosic biomass,

177     that reduces the molecular weight and crystallinity by breaking chemical bonds in cellulose,

178     hemicellulose and lignin (Khan, Labrie, & McKeown, 1986; Kristiani, Effendi, Styarini, Aulia, &

179     Sudiyani, 2016; Lee et al., 2014). Prior to the main trials, several E-beam dosages had been

180     screened in order to find the optimal radiation dosage for the DP adjustment. Pre-hydrolyzed birch

181     kraft pulp and pine kraft paper pulp were selected as model pulps that were treated together with

182     H25 and H50 by E-beam dosages from 5 to 30 kGy. E-beam treatment – especially at such low

183     irradiation intensity – was expected to not alter the chemical compositions of the pulps (Imamura,

184     Murakami, & Ueno, 1972; Kassim et al., 2016; Kristiani et al., 2016). Figure 1 presents the

185     intrinsic viscosity of the original and the E-beam treated kraft pulps as a function of the irradiation

186     dosages. A pronounced decrease in intrinsic viscosity (DP) was visible already at 10 kGy. The

187     viscosity then tended to decrease gradually upon progressive increase of the E-beam dosage. This

188     finding confirmed that E-beam irradiation is a suitable method to reduce the polymer-DP through

189     chain scission (Imamura et al., 1972).

**Figure 1**. The intrinsic viscosity of E-beam treated H25 and H50 samples and a reference birch PHK pulp.

To assess the effects of E-beam treatment on the carbohydrates in more detail, the molecular weight distribution of the E-beam treated pulps was analyzed (Figure S2). Typically, a bimodal molecular weight distribution was obtained for all the measured samples. The results of GPC measurements clearly demonstrated that the high molecular weight domains shifted to lower molar mass, while the molecular weight of the short-chain fraction remained unchanged. This is in agreement with the intrinsic viscosity measurement where the intrinsic viscosity decreases as E-beam dosage increases.

**3.2 Dissolution and dope properties**

Spinning dopes were prepared in [DBNH]OAc with the acid hydrolyzed kraft pulp from H1200 to H200 and E-beam treated (20 kGy) kraft pulps H25 and H50. The rheological properties of the dopes were determined via oscillatory shear measurements yielding the complex viscosity and dynamic moduli as a function of the angular frequency. The crossover point of the dynamic moduli

207  and the zero shear viscosity were calculated using the Cross model and assuming the validity of

208  the Cox-Merz rule (Hummel et al., 2015). In previous studies (Sixta et al., 2015), it was found that

209  stable spinning is possible if the zero shear viscosity of the spin dope is around 30 000 Pa.s and

210  the crossover modulus ranges between 3000 and 5000 Pa at a crossover frequency of around 1 s[-]

211  [1]. Several subsequent studies (Asaadi et al., 2016; Yibo Ma et al., 2015a; A Michud et al., 2014;

212  Anne Michud, Tanttu, et al., 2016) have confirmed these requirements for successful fibre spinning.

213  However, a successful fibre spinning was observed when attempting to spin a spinning dope from

214  an unbleached pulp, of which the rheology was outside the optimal spinning window (Y Ma et al.,

215  2016).

216  Since the molar mass distribution and the DP of the raw material are crucial for the viscoelastic

217  properties of the spinning dope, the selection of the polymer concentration (or spinning

218  temperatures) has to be adjusted in order to meet the above-mentioned dope properties (Anne

219  Michud, Hummel, & Sixta, 2015, 2016). Because of the low intrinsic viscosity of the resulting

220  acid hydrolyzed kraft pulps, H1200 and H1000, a 15 wt% concentration of these pulps in

221  [DBNH]OAc was prepared to adjust the required viscoelastic properties and thus to ensure their

222  spinnability. Contrary to our expectation, these two dopes exhibited a high complex viscosity

223  without a Newtonian plateau within the measured angular frequency range (gel-like power-law

224  dependency). To reduce the dope viscosity, spinning dopes from H800, H500 and H200 were

225  prepared with a polymer concentration of 13 wt%. However, only two of them, the H800 and

226  H500-derived dopes, revealed the expected complex viscosity typical for spinnable solutions

227  (Figure 2A). The zero shear viscosity of the spinning dopes from H200 to H1200 is listed in Table

228  S2. At a low H-factor of H200, the respective dope showed a strong gel-character even at 13 wt%

229  polymer concentration and despite a low pulp intrinsic pulp viscosity. This was attributed to a

230 lignin with a relatively high content of 15%, which is presumably bond to hemicellulose and/or

231 cellulose to form lignin-carbohydrate complexes (LCC). Thus, it can be hypothesized that residual

232 lignin embedded in the cell wall architecture acts as a crosslinker between the carbohydrate

233 polymer chains, which tend to form extended aggregates in solution exhibiting a gel behavior of

234 the resulting dope.
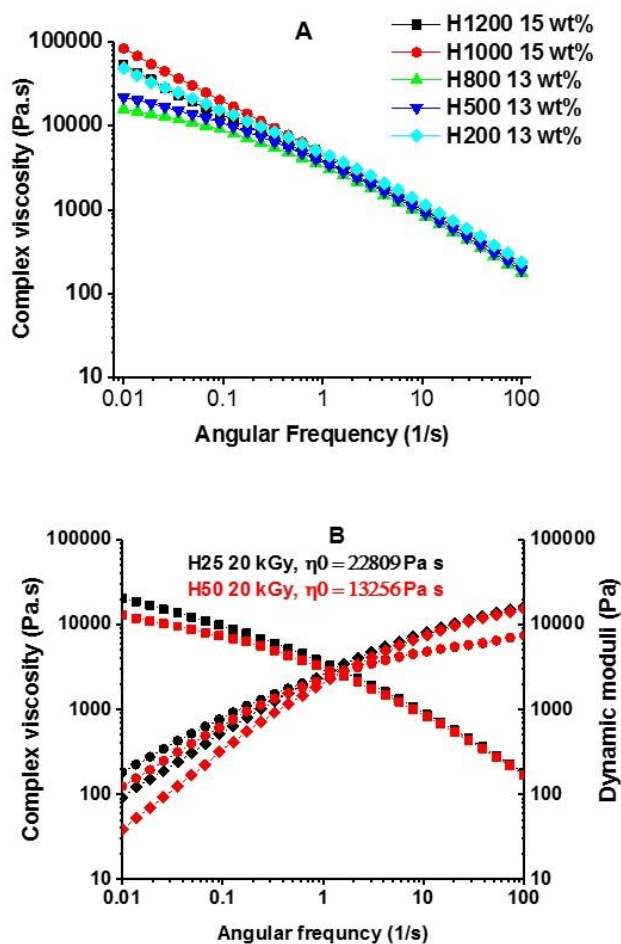


235

236 **Figure 2**. A) Complex viscosity of the spinning dopes from H200 to H1200 at the spinning

237 temperatures. B) Complex viscosity and dynamic moduli of E-beam treated kraft pulps H25 and

238 H50 at 70 ºC. ■: Complex viscosity. ♦: Storage modulus. ●: Loss modulus.

239

240  The E-beam treated birch kraft pulps (20 kGy, H25 and H50) were dissolved in [DBNH]OAc at

241  a polymer concentration of 13 wt%. Figure 2B illustrates the viscoelastic properties of the E-beam

242  treated pulps. Unlike a solution from H200, these two dopes did not show any gel behavior

243  regardless of the high lignin content. This could be explained by the efficient cleavage of the

244  cellulose and lignin chains as well as the LCC bonds by the electron beam irradiation (Bak, 2014).

245  Direct comparison of the viscoelastic properties of the dopes prepared from H25 and H50, revealed

246  a more pronounced solution state for the H50. At high angular frequency complex viscosity and

247  dynamic moduli of the two dopes were almost perfectly superimposed. At low angular frequency

248  the complex viscosity of the H50 dope started to enter the Newtonian plateau whereas the complex

249  viscosity of the H25 dope continues to raise. As a result, the zero shear viscosity of H25 dope was

250  higher than that from the H50 dope.

251

252 **3.3 Dope spinnability and tensile properties of the spun fibres**

253  The spinning performance depends on several factors of which most are connected to the dope

254  rheology. The polymer solution must exhibit the right fluidity to be extruded through the spinneret

255  orifices. Further, a dry-jet wet spinning process demands the stretch of the filaments in the air gap.

256  Hence, the filaments must have a certain visco-elasticity to withstand the draw without rupture.

257  We have thus defined spinnability in terms of accessible draw ratios: DR<2 non-spinnable, 2–8

258  poor, 8–14 good, >14 excellent spinnability. All dopes showed good to excellent spinnability. In

259  the case of acid hydrolyzed kraft pulps, only H1200 showed a relative low spinnability (reflected

260  by the low draw ratio of 8.8). Considering the high cellulose content in H1200, a better spinning

261  performance was expected. Possibly, the high dope viscosity and the relatively high spinning

262  temperature may have limited the spinnability. The solution prepared from the H800 pulp showed

263  the highest spinnability with a maximum draw ratio of 17.7. Surprisingly, the dopes from H200,

264    H50 and H25, which contained large amounts of lignin and hemicellulose, were still spinnable and

265    showed good spinnability (15.9 for H200 and 9.7 for both H25 and 50). Table 2 summarizes the

266    mechanical properties of the spun fibres. The fibre tenacity is closely linked with the cellulose

267    microfibril orientation in the fibre (H P Fink et al., 2001; Kong & Eichhorn, 2005). A high draw

268    ratio results in fibres with more pronounced lateral orientation of the polymer chain, therefore,

269    yields fibres with improved tenacity. Due to the low spinnability, the fibre spun form H1200 dope

270    had the lowest conditioned (32.9 cN/tex) and wet tenacity (19.9 cN/tex) among the fibres from

271    acid hydrolyzed kraft pulps, while the H800 fibre showed the highest conditioned tenacity of 40.2

272    cN/tex and wet tenacity of 29.3 cN/tex due to the excellent spinnability of the dope. The lignin and

273    hemicellulose content do not only affect the spinnability, but also influence the mechanical

274    properties of the spun fibres through their relatively low DP and their inability to orient themselves

275    along the molecular axis. Because the lignin contents in H200, H50 and H25 pulps are significantly

276    higher as compared to the other pulps, the mechanical properties of the resulting fibres were

277    notably reduced. Especially, the fibres spun from the H50 and H25 pulps reveal a conditioned

278    tenacity of only 24.4 and 23.0 cN/tex, which may be explained by a very low cellulose content of

279    56% and 58%, respectively (Table 2).

280

281    **Table 2**. Tensile properties of the spun fibres from H1200 to H200 dopes.

282
283

| Samples | Draw ratio | Titer (dtex) | Dry elongation (%) | Dry tenacity (cN/tex) | Wet elongation (%) | Wet tenacity (cN/tex) |
|---------|-----------|--------------|--------------------|-----------------------|--------------------|-----------------------|
| H25 | 9.7 | 2.02 | 8.1 | 23.0 | 7.7 | 11.1 |
| H50 | 9.7 | 2.14 | 7.4 | 24.4 | 7.0 | 13.7 |
| H200 | 15.9 | 1.71 | 7.6 | 32.1 | 8.8 | 20.1 |
| H500 | 12.4 | 1.78 | 9.0 | 38.1 | 9.2 | 26.1 |
| H800 | 17.7 | 1.43 | 7.7 | 40.2 | 9.7 | 29.3 |
| H1000 | 15.9 | 1.58 | 8.0 | 37.3 | 8.6 | 24.9 |
| H1200 | 8.8 | 2.74 | 9.2 | 32.9 | 9.4 | 19.9 |
| Lyocell | - | 1.3 | 9.5 | 34.3 | - | - |

284

### 3.4 Structural properties of fibres

As stated above, the tensile properties of the fibre are directly connected to the cellulose orientation. The total orientation of cellulose molecules in a fiber matrix can be assessed by means of birefringence measurement. In agreement with the previous studies (Asaadi et al., 2016; Yibo Ma et al., 2015a), the degree of orientation of the fibers increased significantly at low draw ratio and tends to level-off when exceeding a draw ratio of 5. A slight drop in the orientation might occur at higher draw ratio due to relaxation of the cellulose molecules, which is caused by the slippage of cellulose chains and the breakage of the intermolecular hydrogen bonds among the cellulose molecules (Asaadi et al., 2016; Kong & Eichhorn, 2005). Figure 3 shows that the total degree of orientation was affected by both the lignin concentration and the spinnability, characterized by the draw ratio during spinning. Surprisingly, H1200 fibres that could be produced only at relatively low draw ratio showed an overall lower orientation than pulps with a similar composition. In the case of H200, H50 and H25 fibres, having a significantly higher lignin content, the total orientation was notably reduced. The presence of lignin disturbs the highly ordered structure formed by cellulose chains and, thus, reduces the total orientation of the fiber (Kong & Eichhorn, 2005). The development of the degree of orientation is consistent with the tensile properties of the fibres. A reduction of total orientation caused a decrease of the fibre tenacity.
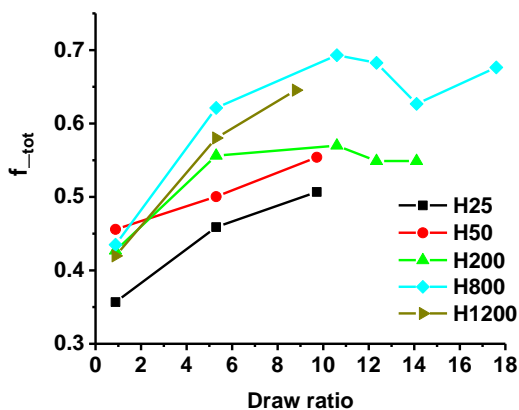
**Figure 3**. Degree of total orientation f_tot of the fibres at selected draw ratios.

The crystallinity and the crystallite size of fibres listed in Table 3 were assessed by XRD measurement. The XRD spectra of selected samples are shown in Figure S3. The crystallinity of the fibres increases upon progressive cooking intensity of pulp production, with the fibre spun from the H1200 pulp having the largest crystallinity of 50%. The increase in the lignin content of the fibres spun from kraft pulps prepared with gradually decreased cooking intensity (from H-factor 200 to H-factor 25) results in a crystallinity drop to 43% and 40% in relation to the total sample, respectively. The crystallite dimensions were assessed in 110, 1-10 and 020 direction and extrapolated by using the Scherrer equation (Leppänen et al., 2011). The crystallite width measured in 110 direction (perpendicular to the cellulose crystal plane) follows the trend of the degree of crystallinity. By contrast, there is no distinct difference observed in the crystalline width in 1-10 direction. However, it has to be noted that the fit quality of the 110 and 1-10 crystallite width suffered from the overlap of the respective peaks. Furthermore, it has been shown that the signals from 110 and 1-10 may include crystal aggregations or less ordered cellulose chains on the surface which result in erroneous values for the crystallite width (Cheng et al., 2011; Maurer, Sax, & Ribitsch, 2013). In general, the crystallite width estimated in 020 direction (sharp peak from 22 to 25° with high intensity in the XRD diffractograms) is more reliable. However, no distinct

15

321 correlation between the 020 crystallite width and the lignin content (i.e. pretreatment intensity)

322 was observed.

323

324 **Table 3**. Crystallinity and crystallite width analyzed by XRD from the H1200, H800, H200, H50

325 and H25 fibres at the highest draw ratio.

| Samples | Draw ratio | Crystallinity index (%) | Crystallite width (nm) | | |
|---|---|---|---|---|---|
| | | | 110 | $1\bar{1}0$ | 020 |
| H25 | 9.7 | 40±3 | 2.6±0.15 | 3.2±0.3 | 5.7±0.8 |
| H50 | 9.7 | 40±3 | 2.9±0.15 | 3.2±0.3 | 6.0±0.3 |
| H200 | 15.9 | 43±3 | 3.4±0.15 | 2.9±0.3 | 5.6±0.3 |
| H800 | 17.7 | 48±3 | 3.8±0.15 | 2.9±0.3 | 5.8±0.3 |
| H1200 | 8.8 | 50±3 | 3.8±0.15 | 3.1±0.3 | 5.5±0.3 |

333

334     Scanning electron microscopy images of the fibres (surfaces and cross sections) were recorded

335 in order to examine their structural alterations along their compositional changes (Figure 4). Indeed,

336 SEM images reveal a significant effect of the pretreatment intensity on the structure of the fibre.

337 When the fibres contained a higher amount of lignin (H25 and H200), the microfibrils became less

338 orientated and voids were clearly visible in the SEM images of the cross section. Consequently,

339 the fibres become more ductile which leads to a loose structure. When the cellulose content

340 increased (H800 and H1200), the orientation of the cellulose microfibrils became more

341 pronounced and the fibre surfaces appeared smooth.

342

**Cross sections**

1) 2)
3) 4)

**Surface**

1) 2)
3) 4)

343
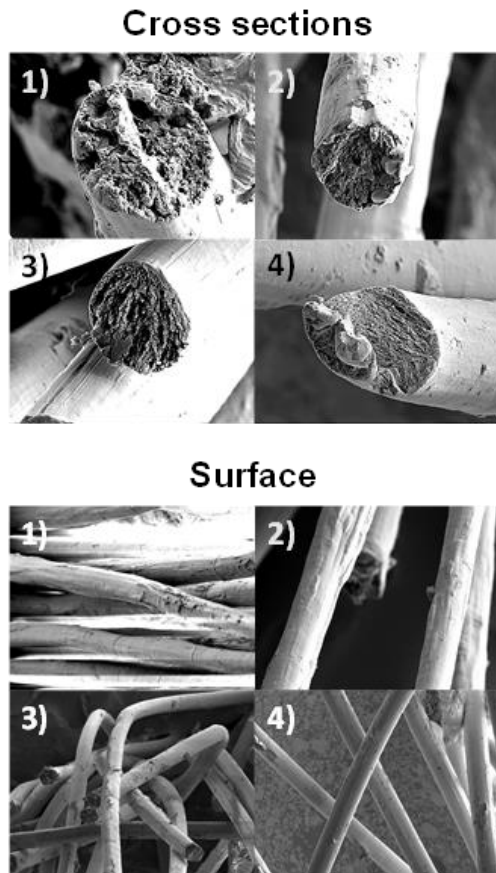
**Figure 4**. SEM images of fibres cross sections (top) and surface (bottom); 1) H25, 2) H200, 3) H800 and 4) H1200.

Dynamic vapour sorption (DVS) studies were conducted to gain further insight into the relationship between the structural and chemical characteristics of the fibers. Water sorption behavior of regenerated cellulosic fibres depends on several factors, e.g. morphology, crystallinity, degree of orientation and the chemical compositions (Bingham, 1964; Kreze & Malej, 2003; Okubayashi, Griesser, & Bechtold, 2004, 2005b, 2005a; Siroka, Noisternig, Griesser, & Bechtold, 2008; Stana-Kleinschek, Ribitsch, Kreže, Sfiligoj-Smole, & Peršin, 2003). It has been shown that Lyocell type fibres absorb a little bit less moisture compared to viscose fibres due to their higher degree of orientation (which is closely related to crystallinity) and more compact structure.

17

354 However, when lignin as a hydrophobic component is present in the fibres it may hamper the

355 moisture absorption as was observed earlier (Yibo Ma et al., 2015a). Figure 5 illustrates the

356 equilibrium moisture sorption and desorption isotherms of tested fibres (a) and shows their

357 hysteresis (b).

358
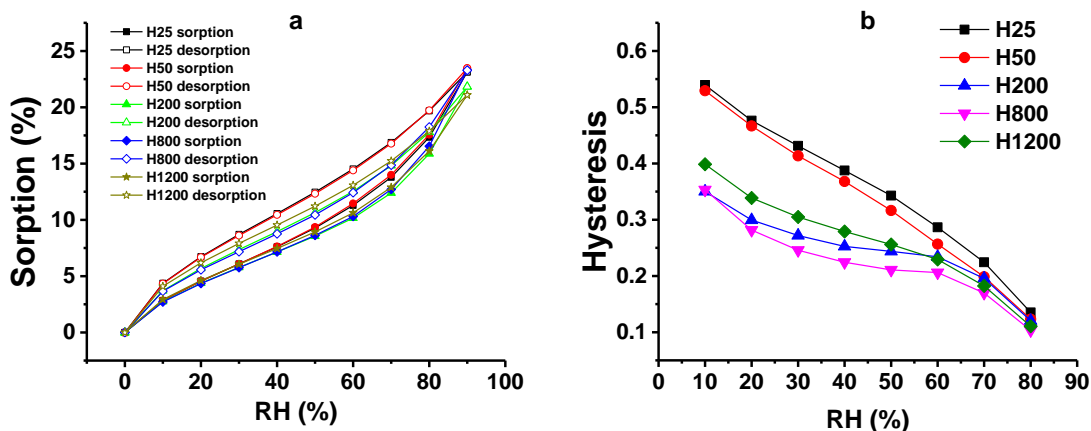


359 **Figure 5**. Equilibrium moisture isotherms of spun fibres (a) and the hystereses of the sorption and

360 desorption isotherms from H25, H50, H200, H800 and H1200 fibres (b).

361
362   Comparing with the previous studies on the DVS of man-made cellulose fibres (Okubayashi et

363 al., 2004, 2005a, 2005b), a similar moisture sorption and desorption development was found with

364 the fibres spun from kraft pulp/ionic liquid dopes, which is typical for cellulosic materials.

365 Contrary to our expectation, lignin did not act as a moisture repellent in these fibres. However, it

366 contributed more to the loss of the fibre orientation together with hemicellulose. Thus, a clear

367 effect of the degree of orientation on the wetting of the fibres was noted. Moreover, the role of the

368 cellulose crystallite size (derived from the 020 reflection) on the monolayer (ML) hydration has

369 been investigated based on the theory proposed by Driemeier (Driemeier & Bragatto, 2013) using

370 the Hailwood-Horrobin (HH) model (Hailwood & Horrobin, 1946; Skaar, 1988) with lignin-free

cellulose I samples. However, no clear relationship between ML water sorption and reciprocal crystallite width could be identified, because of the presence of lignin and different crystal structure in our spun fibres (see ESI section 4, Table S2). Lignin, hemicellulose and the degree of orientation seem to be more dominant factors.

To further exhibit the influence of the chemical composition/total orientation of the spun fibres on the water sorption/desorption (presented as ML water sorption, desorption and their hysteresis), multiple regression analysis was carried out with lignin content, hemicellulose content and total orientation as predictor variables. The multiple regression equations are listed in the ESI, section 4. In this work, the three predictor variables are collinear, from which it is possible to express e.g. the total orientation as a linear combination of the other two variables. Thus, there is no need to estimate the responses of the ML water sorption/desorption for any arbitrary combination of the predictor variables. In this scenario, the total orientation could be used as third predictor and restricted to an interval centered around the value obtained by linearly fitting the total orientation to the other predictors. The responses of ML water sorption/desorption are visualized (shown as contour plots in Figure S3-5), in which lignin and hemicellulose are predictors at different levels of aberration of the total variables. The interpretation of the visualization almost proved that the wetting behavior is largely dependent on the chemical composition and the total orientation of the fibre. According to Figure S3, the ML sorption slightly decreases with the hemicellulose content and increases with the lignin content as well as with the total orientation. Figure S4 allows for a similar interpretation on ML desorption, but with the exception that increasing hemicellulose content causes a slight raise on the ML water desorption. Eventually, Figure S5 reveals that increasing the hemicellulose and lignin content simultaneously increases the hysteresis, whereas the increasing total orientation once again has a decreasing effect. However, it has to be stressed

395    that the five data points are not enough for a compelling regression analysis in three variables.

396    Hence, the regression is rather a means of comprehensively visualizing the observed responses at

397    different values of the predictor variables.

398
399
400    **4.  CONCLUSION**

401    1,5-diazabicyclo[4.3.0]non-5-enium acetate is a promising biopolymer solvent for the

402    production of high quality fibres, not only from costly dissolving pulps but also from low-refined

403    unbleached pulps. In this study, our objective to find a limit in the lignin content was not achieved;

404    even at the highest lignin content the pulp was still spinnable. The fibres showed good to excellent

405    mechanical properties. The spinnability was primarily dependent on the macromolecular integrity

406    of the carbohydrate matrix but not as much on its composition. Contrary to our previous study, the

407    lignin present in the fibre did not render the fibre hydrophobic. However, it reduced the total

408    orientation of the fibre, which leads to a more pronounced wetting of the fibre.

409    Most importantly, E-beam irradiation was identified as an environmentally friendly alternative

410    for DP adjustment and production of fibres from unbleached birch kraft pulp with varying amount

411    of lignin and hemicellulose. Contrary to the DP adjustment with an acid treatment, E-beam

412    irradiation does not yield any material losses.  This increases the overall process economy and

413    environmental sustainability of the Ioncell-F technology. For further work, a milder pre-treatment

414    in combination with E-beam irradiation (which cleaves the LCC bonds) is still necessary to

415    investigate the spinning limitation.

416

## Acknowledgements

## References

Asaadi, S., Hummel, M., Hellsten, S., Härkäsalmi, T., Ma, Y., Michud, A., & Sixta, H. (2016). Renewable High-Performance Fibers from the Chemical Recycling of Cotton Waste Utilizing an Ionic Liquid. *ChemSusChem*, *9*(22), 3250–3258. https://doi.org/10.1002/cssc.201600680

Bak, J. S. (2014). Electron beam irradiation enhances the digestibility and fermentation yield of water-soaked lignocellulosic biomass. *Biotechnology Reports*, *4*, 30–33. https://doi.org///dx.doi.org/10.1016/j.btre.2014.07.006

Bingham, B. E. M. (1964). A study of the fine structure of regenerated cellulose fibers. *Die Makromolekulare Chemie*, *77*(1), 139–152. https://doi.org/10.1002/macp.1964.020770113

Cheng, G., Varanasi, P., Li, C., Liu, H., Melnichenko, Y. B., Simmons, B. A., … Singh, S. (2011). Transition of Cellulose Crystalline Structure and Surface Morphology of Biomass as a Function of Ionic Liquid Pretreatment and Its Relation to Enzymatic Hydrolysis. *Biomacromolecules*, *12*(4), 933–941. https://doi.org/10.1021/bm101240z

Driemeier, C., & Bragatto, J. (2013). Crystallite Width Determines Monolayer Hydration across a Wide Spectrum of Celluloses Isolated from Plants. *The Journal of Physical Chemistry B*, *117*(1), 415–421. https://doi.org/10.1021/jp309948h

Fink, H. P., Weigel, P., Ganster, J., Rihm, R., Puls, J., Sixta, H., & Parajo, J. C. (2004). Evaluation

439     of new organosolv dissolving pulps. Part II: Structure and NMMO processability of the pulps.

440     *Cellulose*, *11*(1), 85–98. https://doi.org/10.1023/B:CELL.0000014779.93590.a0

441 Fink, H. P., Weigel, P., Purz, H. J., & Ganster, J. (2001). Structure formation of regenerated

442     cellulose materials from NMMO-solutions. *Progress in Polymer Science*, *26*(9), 1473–1524.

443     https://doi.org///dx.doi.org/10.1016/S0079-6700(01)00025-9

444 Gübitz, G. M., Stebbing, D. W., Johansson, C. I., & Saddler, J. N. (1998). Lignin-hemicullulose

445     complexes restrict enzymatic solubilization of mannan and xylan from dissolving pulp.

446     *Applied Microbiology and Biotechnology*, *50*(3), 390–395.

447     https://doi.org/10.1007/s002530051310

448 Hailwood, A. J., & Horrobin, S. (1946). Absorption of water by polymers: analysis in terms of a

449     simple model. *Transactions of the Faraday Society*, *42*(0), B092.

450     https://doi.org/10.1039/TF946420B084

451 Hauru, L. K. J., Ma, Y., Hummel, M., Alekhina, M., King, A. W. T., Kilpelainen, I., … Sixta, H.

452     (2013). Enhancement of ionic liquid-aided fractionation of birchwood. Part 1: autohydrolysis

453     pretreatment. *RSC Advances*, *3*(37), 16365–16373. https://doi.org/10.1039/C3RA41529E

454 Hermanutz, F., Meister, F., & Uerdingen, E. (2006). New developmens in the manufacture of

455     cellulose fibres with ionic liquids. *Chemical Fibers International*, *56*, 342–343.

456 Hummel, M., Michud, A., Tanttu, M., Asaadi, S., Ma, Y., Hauru, L. K. J., … Sixta, H. (2015).

457     Ionic liquids for the production of man-made cellulosic fibers: Opportunities and challenges.

458     *Advances in Polymer Science*, *217*, 133-168. https://doi.org/10.1007/12_2015_307

459 Hämmerle, F. M. (2011). The cellulose gap (the future of cellulose fibres). *Lenzinger Berichte*, *89*,

460      12–21.

461    Imamura, R., Murakami, K., & Ueno, T. (1972). Depolymerization of cellulose by electron beam

462      irradiation. *Bulletin of the Institute for Chemical Research, Kyoto University*, *50*(1), 51–63.

463    Jiang, W., Sun, L., Hao, A., & Chen, J. Y. (2011). Regenerated Cellulose Fibers From Waste

464      Bagasse Using Ionic Liquid. *Textile Research Journal*, *81*, 1949–1958.

465    Kassim, M. A., Khalil, H. P. S. A., Serri, N. A., Kassim, M. H. M., Syakir, M. I., Aprila, N. A. S.,

466      & Dungani, R. (2016). Irradiation Pretreatment of Tropical Biomass and Biofiber for Biofuel

467      Production. In *Radiation Effects in Materials* (pp. 329–356). Rijeka: InTech.

468      https://doi.org/10.5772/62728

469    Khan, A. W., Labrie, J. P., & McKeown, J. (1986). Effect of electron-beam irradiation

470      pretreatment on the enzymatic hydrolysis of softwood. *Biotechnology and Bioengineering*,

471      *28*(9), 1449–1453. https://doi.org/10.1002/bit.260280921

472    Kong, K., & Eichhorn, S. J. (2005). Crystalline and amorphous deformation of process-controlled

473      cellulose-II fibres. *Polymer*, *46*(17), 6380–6390.

474      https://doi.org///dx.doi.org/10.1016/j.polymer.2005.04.096

475    Kreze, T., & Malej, S. (2003). Structural Characteristics of New and Conventional Regenerated

476      Cellulosic Fibers. *Textile Research Journal*, *73*(8), 675–684.

477    Kristiani, A., Effendi, N., Styarini, D., Aulia, F., & Sudiyani, Y. (2016). The Effect of Pretreatment

478      by using Electron Beam Irradiation On Oil Palm Empty Fruit Bunch. *Atom Indonesia*, *42*(1),

479      9. https://doi.org/10.17146/aij.2016.472

480    Le, H. Q., Ma, Y., Borrega, M., & Sixta, H. (2016). Wood biorefinery based on gamma]-

481      valerolactone/water fractionation. *Green Chemistry*, *18*(20), 5466–5476.

482      https://doi.org/10.1039/C6GC01692H

483    Lee, B.-M., Lee, J.-Y., Kim, D.-Y., Hong, S.-K., Kang, P.-H., & Jeun, J.-P. (2014).

484      Environmentally-Friendly Pretreatment of Rice Straw by an Electron Beam Irradiation.

485      *Korean Society for Biotechnology and Bioengineering Journal*, *29*(4), 297–302.

486      https://doi.org/10.7841/ksbbj.2014.29.4.297

487    Leppänen, K., Bjurhager, I., Peura, M., Kallonen, A., Suuronen, J.-P., Penttilä, P., … Serimaa, R.

488      (2011). X-ray scattering and microtomography study on the structural changes of never-dried

489      silver birch, European aspen and hybrid aspen during drying. *Holzforschung*, *65*(6), 865–873.

490      https://doi.org/10.1515/HF.2011.108

491    Ma, Y., Asaadi, S., Johansson, L.-S., Ahvenainen, P., Reza, M., Alekhina, M., … Sixta, H. (2015a).

492      High-Strength Composite Fibers from Cellulose–Lignin Blends Regenerated from Ionic

493      Liquid Solution. *ChemSusChem*, *8*(23), 4030–4039. https://doi.org/10.1002/cssc.201501094

494    Ma, Y., Asaadi, S., Johansson, L. S., Ahvenainen, P., Reza, M., Alekhina, M., … Sixta, H. (2015b).

495      High-Strength Composite Fibers from Cellulose-Lignin Blends Regenerated from Ionic

496      Liquid Solution. *ChemSusChem*, *8*(23), 4030–4039. https://doi.org/10.1002/cssc.201501094

497    Ma, Y., Hummel, M., Maattanen, M., Sarkilahti, A., Harlin, A., & Sixta, H. (2016). Upcycling of

498      waste paper and cardboard to textiles. *Green Chemistry*, *18*(3), 858–866.

499      https://doi.org/10.1039/C5GC01679G

500    Maurer, R. J., Sax, A. F., & Ribitsch, V. (2013). Moleular simulation of surface reorganization

501      and wetting in crystalline cellulose I and II. *Cellulose*, *20*(1), 25–42.

502       https://doi.org/10.1007/s10570-012-9835-9

503    Michud, A., Hummel, M., & Sixta, H. (2015). Influence of molar mass distribution on the final

504       properties of fibers regenerated from cellulose dissolved in ionic liquid by dry-jet wet

505       spinning. *Polymer*, *75*, 1–9. https://doi.org///dx.doi.org/10.1016/j.polymer.2015.08.017

506    Michud, A., Hummel, M., & Sixta, H. (2016). Influence of process parameters on the structure

507       formation of man-made cellulosic fibers from ionic liquid solution. *Journal of Applied*

508       *Polymer Science*, *133*(30), n/a. https://doi.org/10.1002/app.43718

509    Michud, A., King, A., Parviainen, A., Sixta, H., Hauru, L., Hummel, M., & Kilpeläinen, I. (2014).

510       Process for the production of shaped cellulose articles.

511    Michud, A., Tanttu, M., Asaadi, S., Ma, Y., Netti, E., Kääriainen, P., … Sixta, H. (2016). Ioncell-

512       F: ionic liquid-based cellulosic textile fibers as an alternative to viscose and Lyocell. *Textile*

513       *Research Journal*, *86*(5), 543–552. https://doi.org/10.1177/0040517515591774

514    Mosier, N., Wyman, C., Dale, B., Elander, R., Lee, Y. Y., Holtzapple, M., & Ladisch, M. (2005).

515       Features of promising technologies for pretreatment of lignocellulosic biomass. *Bioresource*

516       *Technology*, *96*(6), 673–686. https://doi.org/10.1016/j.biortech.2004.06.025

517    Okubayashi, S., Griesser, U. J., & Bechtold, T. (2004). A kinetic study of moisture sorption and

518       desorption on lyocell fibers. *Carbohydrate Polymers*, *58*(3), 293–299.

519       https://doi.org///dx.doi.org/10.1016/j.carbpol.2004.07.004

520    Okubayashi, S., Griesser, U. J., & Bechtold, T. (2005a). Moisture sorption/desorption behavior of

521       various manmade cellulosic fibers. *Journal of Applied Polymer Science*, *97*(4), 1621–1625.

522       https://doi.org/10.1002/app.21871

523 Okubayashi, S., Griesser, U. J., & Bechtold, T. (2005b). Water Accessibilities of Man-made

524 Cellulosic Fibers – Effects of Fiber Characteristics. *Cellulose*, *12*(4), 403–410.

525 https://doi.org/10.1007/s10570-005-2179-y

526 Parviainen, A., King, A. W. T., Mutikainen, I., Hummel, M., Selg, C., Hauru, L. K. J., …

527 Kilpeläinen, I. (2013). Predicting Cellulose Solvating Capabilities of Acid-Base Conjugate

528 Ionic Liquids. *ChemSusChem*, *6*(11), 2161–2169. https://doi.org/10.1002/cssc.201300143

529 Rosenau, T., Potthast, A., Sixta, H., & Kosma, P. (2001). The chemistry of side reactions and

530 byproduct formation in the system NMMO/cellulose (Lyocell process). *Progress in Polymer*

531 *Science (Oxford)*, *26*(9), 1763–1837. https://doi.org/10.1016/S0079-6700(01)00023-5

532 Siroka, B., Noisternig, M., Griesser, U. J., & Bechtold, T. (2008). Characterization of cellulosic

533 fibers and fabrics by sorption/desorption. *Carbohydrate Research*, *343*(12), 2194–2199.

534 https://doi.org///dx.doi.org/10.1016/j.carres.2008.01.037

535 Sixta, H. (2006). Chemical Pulping Processe: Sections 4.2.8–4.3.6.5. In *Handbook of Pulp* (pp.

536 366–509). Weinheim, Germany: Wiley-VCH Verlag GmbH.

537 https://doi.org/10.1002/9783527619887.ch4c

538 Sixta, H., Michud, A., Hauru, L., Asaadi, S., Ma, Y., King, A. W. T., … Hummel, M. (2015).

539 Ioncell-F: A High-strength regenerated cellulose fibre. *Nordic Pulp and Paper Research*

540 *Journal*, *30*(1), 043–057. https://doi.org/10.3183/NPPRJ-2015-30-01-p043-057

541 Skaar, C. (1988). Theories of Water Sorption by Wood. In *Wood-Water Relations* (pp. 86–121).

542 Berlin: Springer Berlin Heidelberg. https://doi.org/10.1007/978-3-642-73683-4_3

543 Stana-Kleinschek, K., Ribitsch, V., Kreže, T., Sfiligoj-Smole, M., & Peršin, Z. (2003). Correlation

of regenerated cellulose fibres morphology and surface free energy components. *Lenzinger Berichte*, *82*, 83–95.

Sun, N., Li, W., Stoner, B., Jiang, X., Lu, X., & Rogers, R. D. (2011). Composite fibers spun directly from solutions of raw lignocellulosic biomass dissolved in ionic liquids. *Green Chemistry*, *13*(5), 1158–1161. https://doi.org/10.1039/C1GC15033B

Sun, N., Rahman, M., Qin, Y., Maxim, M. L., Rodriguez, H., & Rogers, R. D. (2009). Complete dissolution and partial delignification of wood in the ionic liquid 1-ethyl-3-methylimidazolium acetate. *Green Chemistry*, *11*(5), 646–655. http://dx.doi.org/10.1039/B822702K